

RESEARCH INTO TRUCK TRANSMISSION TORSION VIBRATIONS UNDER LONGITUDINAL ACCELERATION

Miroslav Demić¹, Branislav Rakićević², Mikica Jovanović^{2*}, Branko Miličić²

¹ Academy of Engineering Sciences, Belgrade, Serbia

² University of Belgrade, Faculty of Mechanical Engineering, Belgrade, Serbia

The development of a modern motor vehicle is aimed at improving the performance in the field of dynamics (both longitudinal and lateral), economy, safety and ergonomic characteristics. Special attention is paid to passenger comfort. Torsional oscillations in transmission cause longitudinal vibrations of the vehicle, depending on inertial parameters, as well as on stiffness and damping of the transmission. Taking into account the complexity of the problem, it is estimated that it is useful to analyse the impact of the transmission design parameters on the longitudinal (fore and aft) vibrations of freight motor vehicle. For this purpose, the dynamic simulation method was used, and the analysis of the influence of certain constructive parameters on the longitudinal oscillations of the vehicle was performed using the sensitivity function.

Key words: vehicle, transmission, torsional vibration, longitudinal acceleration

INTRODUCTION

One of the dominant aspects of comfort is certainly oscillatory comfort, due to the pronounced effect on the sightings and health of the driver and the passengers. [1-4].

The human being is exposed to vibrations, noise, microclimate, etc. in the vehicle, but this paper will only discuss the longitudinal vibrations. The behaviour of a human body under oscillatory loads depends on the anthropometric parameters, excitation nature and amplitude and frequency of vibration [5]. This problem is complex and is explained in more detail in the literature [1-5].

A specific group of longitudinal oscillations consists of those that are driven by a sudden change in torque of the engine in the event of a sudden deceleration or acceleration. This change causes low frequency torque oscillations in transmission [6-9]. They depend on inertial parameters, as well as on stiffness and damping of transmission, and cause longitudinal vibrations of the vehicle. Taking into account the complexity of the problem, it is estimated that it is useful to analyse the impact of the transmission design parameters on the longitudinal oscillations.

For this purpose, the dynamic simulation method was used, and the analysis of the influence of certain design parameters on the longitudinal vibrations of the vehicle was performed using the sensitivity function [10], which will be discussed in more detail below.

MATHEMATICAL MODEL OF A TRANSMISSION

When modelling the vehicle and its systems models of different structures are used [11-20], in practice the principle is that their complexity covers only those values that are being analysed [5]. This is justified by the

fact that more complex models require the use of a large number of geometric and inertial parameters, which are often not known. The choice of orientation may lead to major errors in the dynamic simulation process, so it is justified to use as simple as possible models. In this sense, in this paper, the transmission scheme shown in Figure 1 is used.

Since the mechanical transmission was the subject of numerous studies [9, 17, 19, 20], this paper presents the research on impact of certain structural parameters of the transmission on the longitudinal vibrations of the vehicle. This was primarily related to the analysis of the impact of the stiffness and damping of the transmission system. Figures 2-5 show the models of transmission subsystems. To bring the mathematical model closer to the real one, it is considered appropriate to include the following analysis; the stiffness of the teeth and the friction between teeth in contact and also, the friction due to the movement of the oil in the gearbox and the final drive. For this reason, the general model (can be applied both the gearbox and the final drive) of the coupled gears is shown in Figure 2 [6].

Figures 3-5 show some more important, parameters, with introduced generalized coordinates. Namely, it is

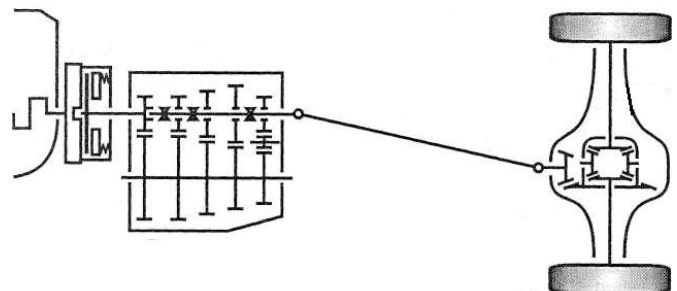


Figure 1: Truck transmission layout

* mjovanovic@mas.bg.ac.rs

considered appropriate to show, in particular, the mechanical coupling models (Figure 3), the gearbox (Figure 4) and the drive axle (Figure 5).

Analyses have shown that in this case it was enough to observe 11 degrees of freedom of movement, since the vibrations of the left and right driven wheel can be considered as identical in the straight line stationary motion of the vehicle.

The impulses of the micro-unevenness on the road were not included in the analysis, as well as the influence of the sprung mass on the longitudinal vibrations of the vehicle. These effects are explained in more detail in the literature [5, 9-20].

It was necessary to define mathematical models for the adopted transmission model, shown in Figures 1-5. This was done using the second-order Lagrange differential equations, whose general form is [21]:

$$\frac{d}{dt} \frac{\partial E_k}{\partial \dot{q}_j} - \frac{\partial E_k}{\partial q_j} + \frac{\partial E_p}{\partial q_j} + \frac{\partial \Phi}{\partial \dot{q}_j} = Q_j,$$

$$j = 1, s,$$

Where:

E_k - kinetic energy,

E_p - potential energy,

Φ - dissipation function,

Q_j - generalized forces,

q_j, \dot{q}_j - generalized coordinates and their velocities

s - number of degrees of freedom of the system movement.

It is obvious that for their application, it was necessary to calculate the kinetic and potential energy, the dissipation

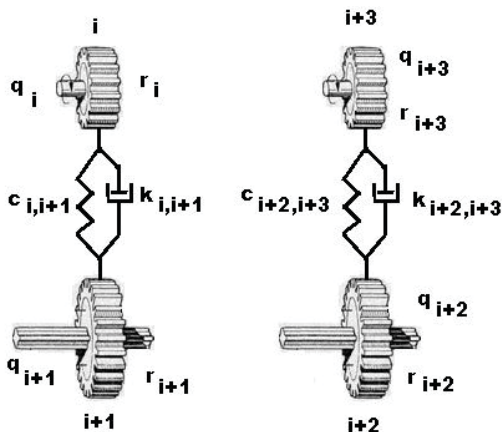


Figure 2: General paired gears model

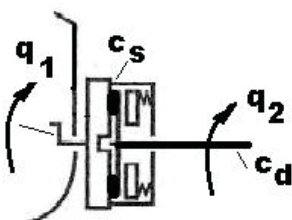


Figure 3: Coupling model

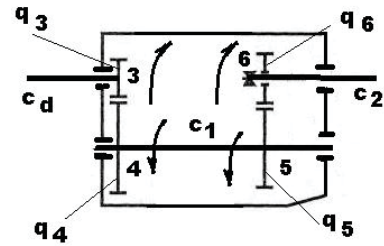


Figure 4: Gearbox model

function and the generalized force of the system, which will be done in the following text.

Energy transformation happens due to deformation of the gear teeth and friction between them. Figure 2 shows the gear pairs of gearbox ($i = 3$) and the final drive ($i = 7$).

The relative deformation of teeth is given by [6]:

$$\Delta_i = r_i q_i - r_{i+1} q_{i+1} \quad (1)$$

Relative speed of the teeth deformation:

$$\dot{\Delta}_i = r_i \dot{q}_i - r_{i+1} \dot{q}_{i+1} \quad (2)$$

Taking into account the gear ratios:

$$i_k = -\frac{q_{i+1}}{q_i} = -\frac{r_i}{r_{i+1}} \quad (3)$$

Where:

q_i, \dot{q}_i - generalized coordinates and generalized speed,

r_i - radius of corresponding gear,

$k = 1, 2$ for the first and second pair of gears in the gearbox, $k = 3, 4$ for gears in the final drive,

i - Gear ratio.

By appropriate transformations of the equation (1-3), we obtain:

$$\Delta_{i,i+1} = 4i_k^2 r_{i+1}^2 q_i, \quad (4)$$

$$\dot{\Delta}_{i,i+1} = 4i_k^2 r_{i+1}^2 \dot{q}_i,$$

Analyses have shown that it is desirable that the kinetic energy of the front wheels be attached to the kinetic energies of the drive wheels, which will include the complete influence of the rotating masses [18]. Taking into account the small diameter of the shafts in coupling,

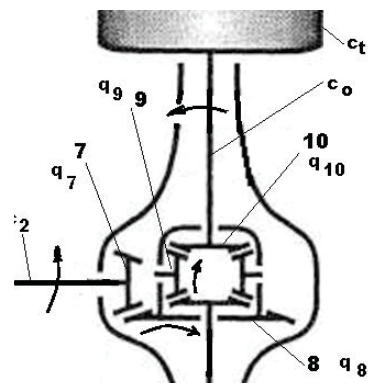


Figure 5: Final drive model

gearbox, final drive and drive shaft, their kinetic energy can be ignored [18]. Bearing that in mind, the kinetic energy of the system is given by the equation:

$$E_k = 0.5I_z \dot{q}_1^2 + 0.5I_3 \dot{q}_3^2 + 0.5I_4 \dot{q}_4^2 + 0.5I_5 \dot{q}_5^2 + 0.5I_6 \dot{q}_6^2 + 0.5I_7 \dot{q}_7^2 + 0.5I_8 \dot{q}_8^2 + 0.5I_9 \dot{q}_9^2 + I_{10} \dot{q}_{10}^2 + 2I_{11} \dot{q}_{11}^2 \quad (5)$$

Bu using gear ratios ik (3), and combining equations 4 and 5, we obtain:

$$E_k = 0.5I_z \dot{q}_1^2 + 0.5(I_3 + i_1^2 I_4) \dot{q}_3^2 + 0.5(I_5 + i_2^2 I_6) \dot{q}_5^2 + 0.5(I_7 + i_3^2 I_8) \dot{q}_7^2 + 0.5(I_9 + 2i_4^2 I_{10}) \dot{q}_9^2 + 2I_{11} \dot{q}_{11}^2 \quad (6)$$

Where:

$I_z, I_3, I_5, I_6, I_7, I_8, I_{10}, I_{11}$ - moments of inertia of the flywheel, the gears and drive wheels, respectively,

$i_1 - i_4$ - gear ratios of corresponding gear pairs

q_i - generalized velocities (Figures 2-5).

Research has shown that the potential energy of the couplings, shafts and tires can be simplified and represented by linear functions of corresponding deformations [6,20]. Given the simplification introduced, the potential energy of the system (including the deformation of the gear teeth equation 4) is given by the equation:

$$E_p = 0.5c_s (q_2 - q_1)^2 + 0.5c_d (q_3 - q_2)^2 + 0.5c_1 (q_5 - q_4)^2 + 0.5c_2 (q_7 - q_6)^2 + 0.5c_3 (q_9 - q_8)^2 + c_u (q_{11} - q_{10})^2 + 2c_{34} i_1^2 r_4^2 q_3^2 + 2c_{56} i_2^2 r_6^2 q_5^2 + 2c_{78} i_3^2 r_8^2 q_7^2 + 2c_{910} i_4^2 r_{10}^2 q_9^2 \quad (7)$$

After the introduction of the appropriate transmission relations (3) and combining equations, we obtain:

$$E_p = 0.5c_s (q_2 - q_1)^2 + 0.5c_d (q_3 - q_2)^2 + 0.5c_1 (q_5 + i_1 q_3)^2 + 0.5c_2 (q_7 + i_1 q_5)^2 + 0.5c_3 (q_9 + i_3 q_7)^2 + 0.5c_u (q_{11} + i_4 q_9)^2 + 2c_{34} i_1^2 r_4^2 q_3^2 + 2c_{56} i_2^2 r_6^2 q_5^2 + 2c_{78} i_3^2 r_8^2 q_7^2 + 2c_{910} i_4^2 r_{10}^2 q_9^2 \quad (8)$$

$$\frac{1}{c_u} = \frac{1}{c_o} + \frac{1}{c_t} \quad (9)$$

where:

c_u, c_o, c_t - the equivalent torsional rigidity of the drive shaft, the torsional rigidity of the drive shaft, and the tangential stiffness of the tire, respectively,

$c_s, c_d, c_1, c_2, c_3, c_{34}, c_{56}, c_{78}, c_{910}$ - torsional rigidity of the couplings, shafts to gearbox, gearbox shafts, propeller shafts, drive shafts, teeth between the respective gear pairs (Figure 2-4), respectively,

r_i - radius of the respective gears,

$i_k - k=1-4$ corresponding gear ratio in the gearbox, or in the final drive.

This paper introduced a simplification of the dissipation function due to tooth friction and oil movement as a linear function, based on the expression (2-4), dissipation function is given by the equation:

$$\Phi = 2k_{34} i_1^2 r_4^2 \dot{q}_3^2 + 2k_{56} i_2^2 r_6^2 \dot{q}_5^2 + 2k_{78} i_3^2 r_8^2 \dot{q}_7^2 + 2k_{910} i_4^2 r_{10}^2 \dot{q}_9^2 \quad (10)$$

Where:

$k_{34}, k_{56}, k_{78}, k_{910}$ - gearbox and final drive damping coefficients (including friction between teeth, and friction due to oil movement).

Generalized forces are given by the equations:

$$Q_1 = M_e$$

$$Q_{11} = -(m r_d \ddot{q}_{11} + m g f \cos(\alpha) + m g \sin(\alpha) + K A q_{11}^2) \frac{r_d}{\eta_u} \quad (11)$$

where:

m - mass of the vehicle,

r_d - dynamic radius of drive wheels,

g - gravitational acceleration,

α - longitudinal inclination of the road,

K - drag resistance coefficient,

A - vehicle frontal area,

η_u - the overall efficiency of the transmission.

Differential equations of motion are defined using the Lagrange equations of the second order:

$$\ddot{q}_1 = \frac{M_e + c_s (q_2 - q_1)}{I_z} \quad (12)$$

$$c_s (q_2 - q_1) = c_d (q_3 - q_2) \quad (13)$$

$$\ddot{q}_3 = - \frac{c_d (q_3 - q_2) + c_1 i_1 (q_5 + i_1 q_3)}{I_3 + i_1^2 I_4} + \frac{4c_{34} i_1^2 r_4^2 q_3 + 4k_{34} i_1^2 r_4^2 \dot{q}_3}{I_3 + i_1^2 I_4} \quad (14)$$

$$\ddot{q}_5 = - \frac{c_1 (q_5 + i_1 q_3) + c_2 i_2 (q_7 + i_2 q_5)}{I_5 + i_2^2 I_6} + \frac{4c_{56} i_2^2 r_6^2 q_5 + 4k_{56} i_2^2 r_6^2 \dot{q}_5}{I_5 + i_2^2 I_6} \quad (15)$$

$$q_5 + i_2 q_4 = q_6 q_5 \quad (16)$$

$$\overset{\infty}{q}_7 = - \frac{c_2(q_7 + i_2 q_5) + c_3 i_3 (q_9 + i_3 q_7)}{I_7 + i_3^2 I_8} \quad (17)$$

$$\frac{+4c_{78} i_3^2 r_8^2 q_7 + 4k_{78} i_3^2 r_8^2 \overset{g}{q}_7}{I_7 + i_3^2 I_8},$$

$$\overset{\infty}{q}_9 = - \frac{c_3(q_9 + i_3 q_7) + 2c_u i_4 (q_{11} + i_4 q_9)}{I_9 + 2i_4^2 I_{10}} \quad (18)$$

$$\frac{+4c_{910} i_4^2 r_{10}^2 q_9 + 4k_{7910} i_3^2 r_{10}^2 \overset{g}{q}_9}{I_9 + 2i_4^2 I_{10}},$$

$$\overset{\infty}{q}_{11} = - \frac{2c_u (q_{11} + i_4 q_9) +}{4I_t + m(r_d^2 / \eta_u)} \quad (19)$$

$$\frac{(r_d / \eta_u)(mg \cos(\alpha) + mg \sin(\alpha) + KA \overset{g}{q}_{11}^2)}{4I_t + m(r_d^2 / \eta_u)},$$

where are:

M_e - engine torque,

$\overset{\infty}{q}_i$ - acceleration of generalized coordinates.

DYNAMIC SIMULATION AND DATA ANALYSIS

Equations 2 and 5 introduce additional links between the system parameters, while equations 1, 3, 4,6,7,8 describe the torsional vibrations of the system. An analysis of the differential equations describing the torsional vibrations of the vehicle shows that they are coupled, non-linear (due to air resistance), with constant coefficients and random excitation (engine torque). Therefore, they had to be transformed into a set of differential equations of the first order, solved numerically by the Kuta-Merson method [22], with an initial time step of 0.01 s, at 4096 points. This enabled an analysis of the vehicle motion of 40.96 s, which is sufficient when considering the engine's excitation function [9]. On the other hand, this provided an analysis at an interval of 0.024 to 50 Hz, which is acceptable when considering the vehicle oscillatory comfort [5]. In doing so, the "bias" was 0.001, the auto spectrum error was 0.1 and the error of calculation of the cross - spectrum 0.18, which is acceptable for the observed technical system [23].

The longitudinal acceleration of the vehicle (20), due to torsional vibration transmissions, are calculated according to the equation:

$$a = r_d \overset{\infty}{q}_{11}. \quad (20)$$

It is shown that transmission torsion vibration is highest during non-stationary driving, i.e. during short accelerations [21]. Engine modelling in such cases is very complicated [8]. For this reason, it is appropriate that its character is idealized and displayed a "delta" function which can serve to describe the engine torque character of short-term acceleration of the vehicle (Figure 6) [24].

Dynamic simulation was carried out on a horizontal path, with the parameters of the truck shown in Table 1.

Table 1: Parameters of the observed truck

c_s , [Nm/rad]	14300
c_1 , [Nm/rad]	500000
c_2 , [Nm/rad]	693000
c_3 , [Nm/rad]	500000
c_t , [Nm/rad]	3200000
c_o , [Nm/rad]	250000
c_{34} , [Nm/rad]	5000
c_{56} , [Nm/rad]	5000
c_{78} , [Nm/rad]	5000
c_{910} , [Nm/rad]	5000
k_{34} , [Nsm/rad]	6000
k_{56} , [Nsm/rad]	6000
k_{78} , [Nsm/rad]	7000
k_{910} , [Nsm/rad]	7000
z , [kgm ²]	3.73
I_p , [kgm ²]	18.5
I_3 , [kgm ²]	2.5
I_4 , [kgm ²]	4
I_5 , [kgm ²]	4
I_6 , [kgm ²]	2.5
I_7 , [kgm ²]	2.5
I_8 , [kgm ²]	4
I_9 , [kgm ²]	2.5
i_1 , [-]	4.5
i_2 , [-]	4.5
i_3 , [-]	3
i_4 , [-]	2
r_4 , [m]	0.15
r_6 , [m]	0.3
r_8 , [m]	0.15
r_{10} , [m]	0.3
m , [kg]	18895
M_{emax} , [Nm]	825
M_{emin} , [Nm]	150
η_u , [-]	0.88
F , [-]	0.01
G , [m/s ²]	9.81
KA , [Ns ² /m ²]	0.75

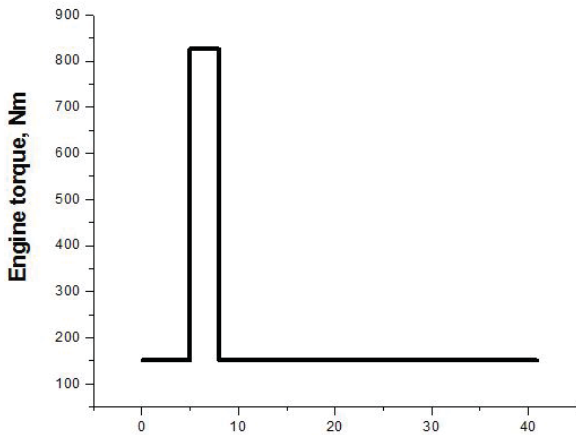


Figure 6: An idealized display of the torque of the engine in case of sudden short-term acceleration of the vehicle

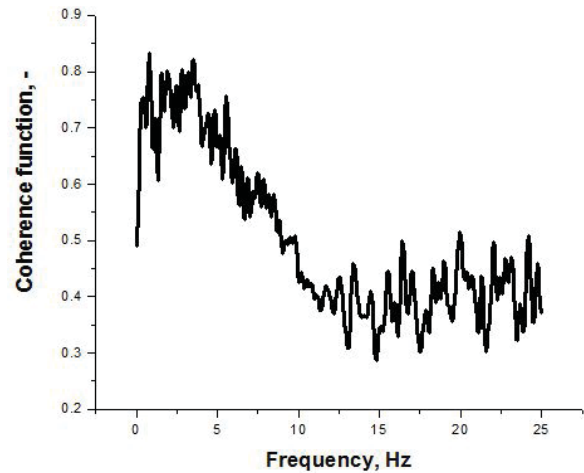


Figure 8: Function of basic coherence

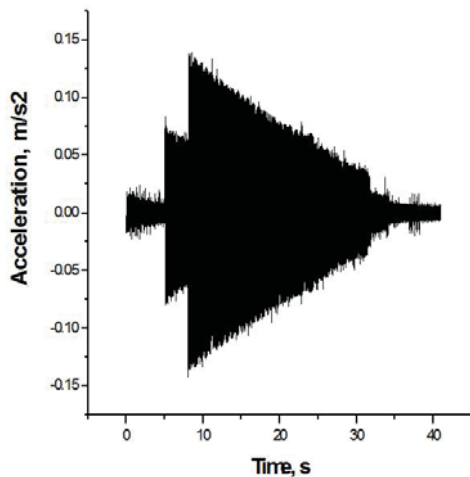


Figure 7: The longitudinal acceleration of the vehicle in short-term change of engine torque

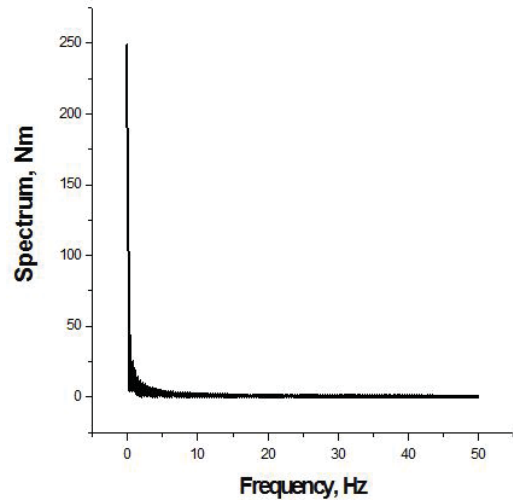


Figure 9: Engine torque amplitude spectrum

Based on the parameters in Table 1 and the equations(1-10), the longitudinal acceleration of the vehicle is calculated, shown in Figure 7.

By analysing Figure 7 it can be seen that the longitudinal acceleration varies with the engine torque. Namely, during a stationary driving straight up to the $t_{min} = 5$ s, the torsional vibration of drive wheels show a trend of calming. With a sudden increase in engine torque from $M_{emin} = 150$ to $M_{emax} = 825$, Nm, their magnitude gets higher, but between $t_{min} = 5$ and $t_{max} = 8$, s, it calms down. After a sudden change of the torque from $M_{emax} = 825$ to $M_{emin} = 150$ Nm, acceleration increases very much, while at further movement they decrease at a constant speed.

In order to carry out a more detailed analysis of the influence of the design parameters of the transmission on the longitudinal vibrations of the vehicle, the function of ordinary coherence between the engine torque and the longitudinal acceleration of the vehicle was calculated. For this purpose, the developed “Demparcoh” program was used and the results are shown in Figure 8.

From Figure 8 it is obvious that the coherence function is higher in the region up to about 5 Hz, which shows

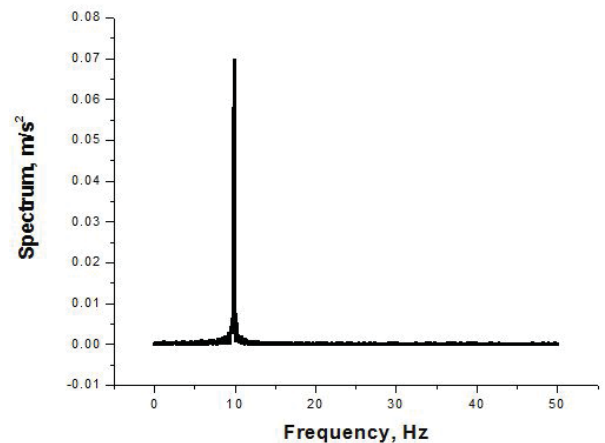


Figure 10: Acceleration spectre

that there is a stronger statistical relation of the observed parameters in this area. Above that frequency, the coherence function decreases, indicating the existence of nonlinearity in the system [23].

Engine torque and vehicle acceleration spectra were calculated using the developed “Analsigdem” program. The results are shown in Figures 9 and 10. It is obvious that the torque spectrum of the motor coupled in Fig. 6.

has the highest amplitudes in the low frequency range (0.146 Hz). On the other hand, the longitudinal accelerations shown in Figure 7 have the highest amplitudes at a frequency of 9.86 Hz.

In order to test at which frequencies these parameters have the strongest statistical relation, the cross-spectrum shown in Figure 11 was calculated.

Analysis of Figure 11 shows that the highest amplitude values are in the low frequency range (0.146 Hz) and at the frequency of 9.86 Hz, which could be expected, based on the character of the auto spectra shown in Figures 9 and 10.

It is also considered useful to calculate the transfer function of the system, Figure 12. Analysing the data from Figure 12, it can be found that the highest peaks are at very low frequencies (0.0976 Hz), while frequencies 1.46, 2.49 and 3.46 Hz, corresponds to lower peak values. These peaks indicate the position of the resonant frequencies of the transmission subsystem.

Analysis have shown that it is useful to calculate the sensitivity functions for the stiffness and damping parameters of the observed vehicle transmission [10]. For illustration purposes, Figures 13 and 14 show some sensitivity functions. An analysis of all the calculated sensitivity functions, partially shown in Figures 13 and 14, revealed that the observed vehicle transmission parameters have approximately the same effect on the vehicle's longitudinal vibrations, which is logical, since vehicle transmission is a system with serial connected elements.

Therefore, it was considered appropriate to carry out a more detailed analysis of all the calculated sensitivity functions. Data on the minimum, medium (starting) and maximum values of the observed stiffness and transmission damping parameters are presented in Table 2. Also, the maximum values of the sensitivity functions for the observed parameters are given, as well as the values of the parameters at which they occur.

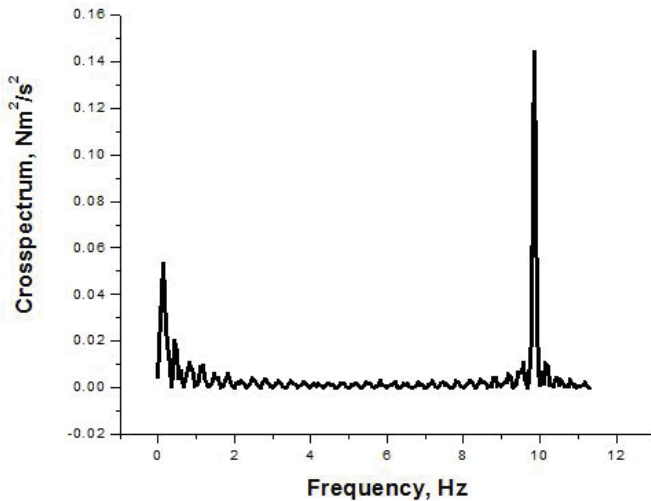


Figure 11: Cross-spectrum

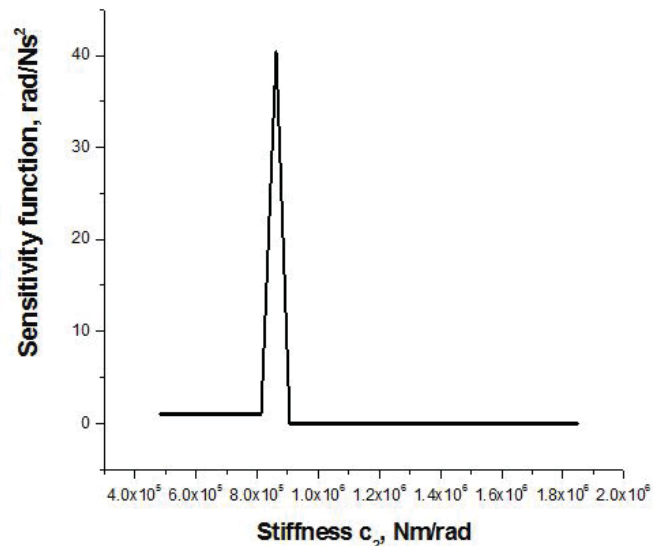


Figure 13: Sensitivity function c_2

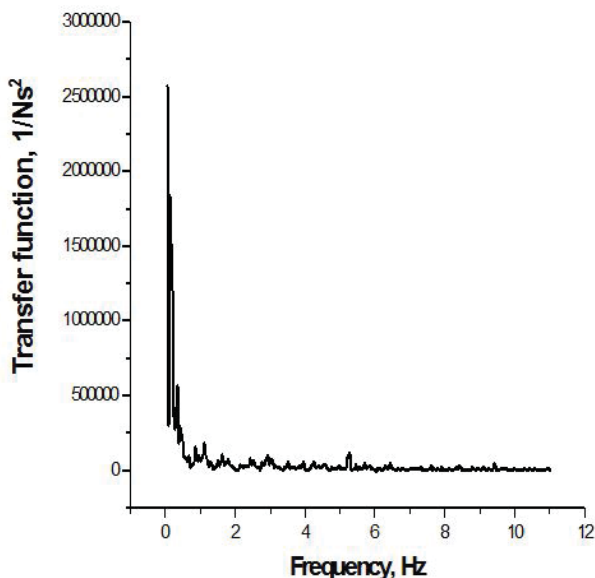


Figure 12: Transfer function

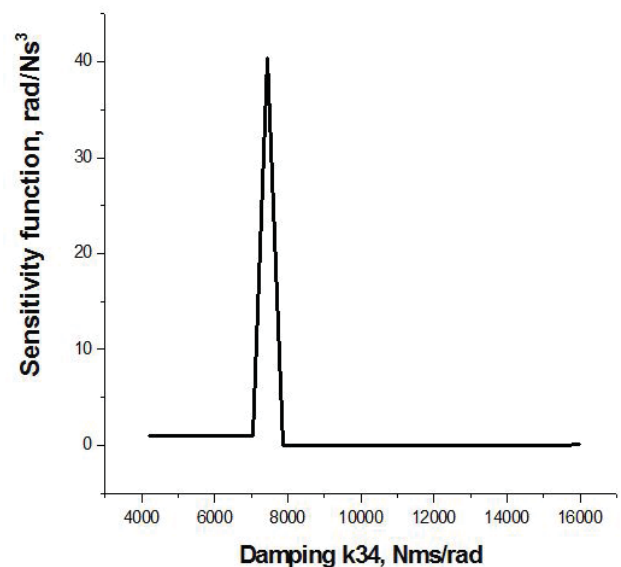


Figure 14: Sensitivity function k_{34}

Table 2: Parameters of sensitivity function

Parameter $c, \text{Nm/rad}$ $k, \text{Nms/rad}$	Minimum value	Starting value	Maximum value	Maximum value of sensitivity function	Parameter at that value
c_1	350000	500000	700000	40.33333187950767	620967
c_2	485100	693000	970200	40.33333222946309	860661
c_3	350000	500000	700000	40.33333186229384	620967
c_{34}	3500	5000	7000	40.33318706562991	6209
c_{56}	3500	5000	7000	40.33318715383798	6209
c_{78}	3500	5000	7000	40.33318758402521	6209
c_{910}	3500	5000	7000	40.33317993158095	6209
c_s	10010	14300	20020	40.33331271039408	17759
c_u	162318	231884	324637	40.33333016018359	28798
k_{34}	4200	6000	8400	40.33321165583845	7451
k_{56}	4200	6000	8400	40.33321165583845	7451
k_{78}	4900	7000	9800	40.33322960856957	8693
k_{910}	4900	7000	9800	40.33317658515675	8693

Note: Dimensions of the sensitivity function * rad/Ns^2 , ** rad/Ns^3

Analysis of the data in Table 2 shows that different initial parameter values led to very close maximum values of the sensitivity functions. However, these values do not occur at the limit or initial values of the parameters (the sixth column of the table), which indicates that there is a sensitivity of longitudinal acceleration of the vehicle to changes in stiffness and damping of the system.

CONCLUSION

Based on the performed research, it is possible to conclude that the set model provided a realistic analysis of the influence of the design parameters of the transmission on the longitudinal accelerations of the freight motor vehicle, so that it, as well as the developed data analysis procedure, can be used in the initial stages of designing the transmission of freight motor vehicles.

ACKNOWLEDGEMENT

Presented results are part of a project financed by the Serbian Ministry of Education, Science and Technological Development (Project TR 35045 - "Scientific-Technological support to Enhancing the Safety of Special Road and Rail Vehicles", project leader - prof. dr Vladimir Popović).

REFERENCES

1. Demić, M. et al. (2002). Some aspects of the investigation of random vibration influence on ride comfort. *Journal of Sound and Vibration*, vol.1, 253, pp. 109-129.
2. Demić, M., Lukić, J.(2008). Human Body Under Two-Directional Random Vibration. *Journal of Low Frequency Noise, Vibration and Active Control*, vol. 27, no. 3,185-201.
3. Demić, M., Lukić, J.(2009). Investigation of the transmission of fore and aft vibration through the human body. *Applied Ergonomics XXX*, pp. 1-8.
4. Griffin, M.J. (1990). *Handbook of Human Vibration*. Academic Press, London.
5. Demić, M. (1997). Optimization of oscillatory systems of motor vehicles (in Serbian). Faculty of Mechanical Engineering, Kragujevac.
6. Grzegorz, L. et al. (2005). Vibration in Gear System. *Haos, Solitons and Fractals*, vol. 16, no. 5, 795-800.
7. Ryzhikov, V.A. et al. (2015). Dynamic Damping Torsional Vibrations in the Transmission of Rear-Wheel Drive and all-Wheel Drive Vehicles. *ARNP Journal of Engineering and Applied Sciences*, vol. 10, no. 12, 5334-5337.
8. Kaminski, E. (1983). *Vehicle theory* (in Polish), Wydawnictwa komunikacji i łączności, Warszawa.
9. Sakota, Z.(2005). Impact of drive scheme on longitudinal oscillations of freight motor vehicles (in Serbian). Doctoral thesis, Faculty of Technical Sciences, Novi Sad.
10. Saltelli, A. et al. (2008). *Global Sensitivity Analysis: The Primer*. John Wiley & Sons.
11. Abe, M., Manning, W. (2009). *Vehicle handling Dynamics*. Butterworth-Heinemann, Elsevier, Amsterdam, Boston.

12. Ellis, J. R. (1973). Vehicle Dynamics. Business Books, London.
13. Gillespie, T. (1992). Fundamentals of vehicle Dynamics. SAE International, Warrendale.
14. Milliken, W., Milliken, D. (1995), Race Car Vehicle-Dynamics. SAE International, Warrendale.
15. Mitschke, M. (1972). Dynamics of motor vehicles (in German). Springer Verlag, Berlin.
16. Genta, A. (2003). Motor Vehicle Dynamics – Modelling and Simulation. World Scientific Publishing, Singapore.
17. Wang, M. (2002). Design and torsional vibration analysis of a complex vehicle powertrain system test rig. 14th International Conference on vibration Engineering, p. 303-309.
18. Demic, M. Lukic, J.(2010). Motor Vehicle Theory (in Serbian). Monograph, Faculty of Mechanical Engineering, Kragujevac.
19. Farshidianfar, A. (2011). Optimization of the high-frequency torsional vibration of vehicle driveline systems using genetic algorithms. Proceedings of the Institution of Mechanical Engineers, Part K: Journal of Multi-body Dynamics, vol. 216, no. 3, 249-262.
20. Nestorides, E. J. (1958). A handbook on torsional vibration. University Press, Cambridge.
21. Pars, L. (1971). A Treatise an Analitic Dynamics. Heinemann, London.
22. Mondal, S.P. Roy, S. Das, B. Mahata, A. Numerical Solution of First Order Linear Differential Equations in Fuzzy Environment by Modified Runge-Kutta Method and Runga-Kutta-Merson-Method under generalized H-differentiability and its Application in Industry. International Journal of Differential Equations. Preprints 2017, 2017120119 (doi: 10.20944/preprints201712.0119.v1).
23. Bendat J. S. and Piersol A.G. (2010). Random Data-Analysis and Measurement Procedures (4th ed.), John Wiley & Sons Inc., Hoboken.
24. Fan, J. (1994). Theoretical and experimental studies on Laeng's oscillations of PKV (Bucking). Doctoral dissertation, TU Braunschweig.

Paper submitted: 13.09.2019.

Paper accepted: 06.03.2020.

This is an open access article distributed under the CC BY-NC-ND 4.0 terms and conditions.